

PUNCTURE DISCHARGES IN SURFACE DIELECTRICS AS
CONTAMINANT SOURCES IN SPACECRAFT ENVIRONMENTS⁺

E. J. Yadlowsky, R. C. Hazelton, and R. J. Churchill
Colorado State University
Fort Collins, CO 80523

ABSTRACT

Spacecraft in geosynchronous orbits are known to become charged to large negative potentials during the local midnight region of the satellite orbit. This surface charging results in electrical discharges which can cause electrical interference with on-board electronic systems. The discharges also constitute a source of contamination for spacecraft sensors and thermal control surfaces because of the transport of charged and uncharged discharge products from the site of the electrical discharge. Such discharges have been studied in the present work by the electron beam irradiation of dielectric samples in a vacuum environment. In addition to static measurements and photographic examination of the puncture discharges in the Teflon samples, the transient characteristics of the electrical discharges are determined from oscillographs of voltage and current and by charged particle measurements employing a biased Faraday cup and a retarding potential analyzer. Using these latter techniques, studies of angular and energy distributions of charged particles have indicated an initial burst of high energy electrons (5×10^{13} per discharge at energies greater than

⁺ Sponsored by NASA Grant No. NSC-43145.

3000 eV) followed by a less intense burst of lower energy negative particles. Positive ions are emitted from the discharge site in an initial high velocity burst followed by a lower velocity burst tentatively identified as carbon. The fact that these particles are measured some 15 cm from the discharge site dramatically indicates the extent to which the discharge constituents may contaminate the satellite environment with particulate deposition and radio frequency noise signals.

1.0 INTRODUCTION

The occurrence of electrical discharges on the surfaces of satellites which penetrate the magnetospheric plasmas is now recognized by spacecraft designers as a technological problem of not insignificant difficulty. For example, the ATS-5 and ATS-6 satellite data revealed the existence of particle fluxes which cause negative surface potentials as high as 20 kV. The spacecraft charging phenomena and the resultant deleterious effects are described in a number of publications and reports.¹⁻³

Under a research grant from NASA (NSG-3145) Colorado State University has undertaken a program wherein the spacecraft charging phenomenon is simulated in a laboratory vacuum chamber by irradiating suitable dielectric targets with an electron beam operating at accelerating potentials from 0-34 kV. A circular Teflon sample is mounted on an annular ring and is enclosed by a grounded aluminum box whose entrance aperture assures that the edges of the Teflon sample are not directly irradiated by the electron beam. This arrangement facilitates the study of particle emission and material damage on both the front and

1. Spacecraft Charging by Magnetospheric Plasmas, (Progress in Astronautics and Aeronautics, Vol. 47) A. Rosen, ed., Cambridge, Mass., MIT Press (1976).
2. Proceedings of the Spacecraft Charging Technology Conference, eds. C. P. Pike and R. R. Lovell, Air Force Geophysics Laboratory (1977).
3. "Space Radiation Effects (Session D of the Annual Conference on Nuclear and Space Radiation Effects," IEEE Transactions on Nuclear Science, NS-24 (No. 6):2244-2304 (1977).

back surfaces of the Teflon sample. Measurements are made of electron beam charging current, charging time, and surface voltage under static conditions while oscillographs in conjunction with transient current probes, fast response potential dividers, loop antennas, photomultipliers and charged particle detectors record the transient nature of the electrical discharges. The physical appearance of the self-luminous electrical discharges is recorded with time-integrated photography, and the resultant damage to the dielectric surface as well as the sites of discharge punctures through the dielectric layer are examined by means of scanning electron beam micrographs. The charged particles emanating from the site of the puncture-type discharges have been measured with biased Faraday cups and retarding potential analyzers.

The most prominent damage feature revealed by the photographs is the existence of crater-like punctures, some 0.06 mm in diameter, through the Teflon layer from the front surface to the silver layer which coats the back surface of the sample. Puncture-type breakdowns occur in one mil Teflon samples at an electron beam voltage of 10 kV, whereas 3 mil Teflon samples break down at a 24 kV electron beam voltage. These values are to be compared with the 10-20 kV negative potentials to which spacecraft surfaces become charged.

Preliminary results indicate that both electrons and positive ions are emitted from the electrical discharge and that significant quantities of heated Teflon are transported from the discharge site to the nearby dielectric surfaces. Angular and energy distributions of charged par-

ticles have indicated an initial burst of high energy electrons with energies in excess of 3000 eV and $\sim 5 \times 10^{13}$ electrons emitted per electrical discharge. This is followed some 5 μ sec later by a less intense burst of lower energy (< 85 eV) negative particles. Positive ions are also emitted from the discharge site in an initial high velocity burst followed by a lower velocity burst of ions tentatively identified as carbon.

In the remainder of this paper the experimental system is discussed briefly. This is followed by a description of the experimental techniques and conditions of particular interest in the area of spacecraft contamination. Results are given for puncture discharges and a wide range of charged particle emissions. Tentative identification of several potential spacecraft contaminants is made.

2.0 EXPERIMENTAL SYSTEM

The spacecraft charging phenomenon is simulated in a vacuum chamber by irradiating a dielectric target with a high-energy electron beam. It is convenient to discuss the total system relative to the schematic diagram shown in Fig. 1.

The simulation chamber consists of a 30 cm diameter cylindrical glass tube about 1 meter in length. Four cylindrical ports 15 cm in diameter located at the central section of the tube provide outlets for vacuum ports, introduction of electrical and photographic measurement systems and the installation of target assemblies. The electron beam

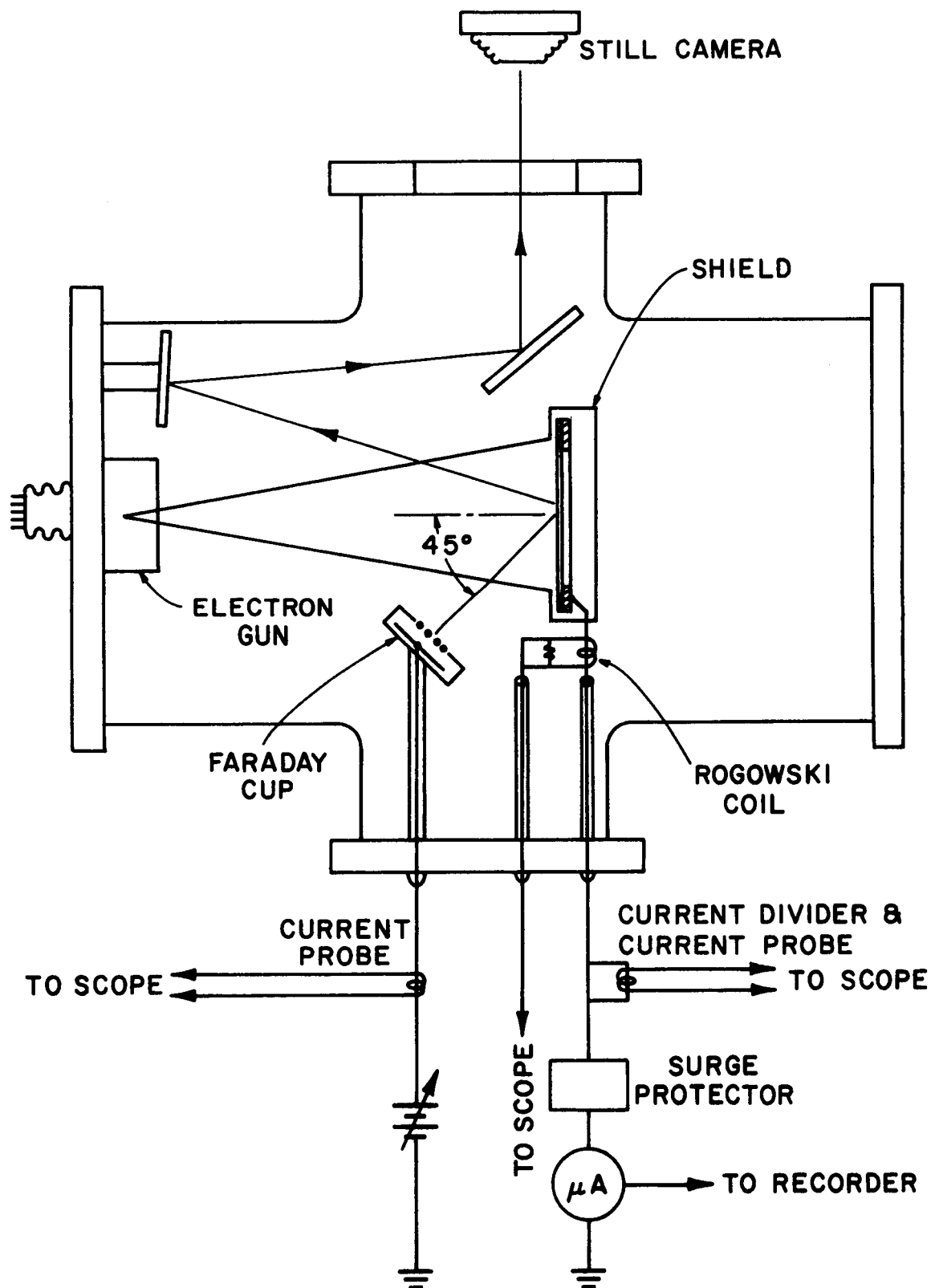


Figure 1. Spacecraft Charging Simulator and Measurement System.

gun is located at one end of the 30 cm diameter cylinder and generates an axial electron beam to the centrally-located target area. Base pressures of 10^{-7} Torr are possible using a 10 cm diameter oil diffusion pump system.

To simulate the spacecraft charging the dielectric targets are bombarded with a mono-energetic electron beam having an acceleration potential from 0 to 34 kV and a beam current density at the target location of 0-5 nA/cm². The divergent electron beam is generated by a directly-heated filament and a grounded, spherical accelerating grid. Beam forming electrodes and the cathode are negatively biased with respect to the grounded accelerating electrode. Uniformity of the electron beam over the target area is about 25% for a 10 cm diameter target located 50 cm from the electron beam gun.

The silver-backed dielectrics used in the irradiation process are mounted on various target assemblies at the center of the four-port region of the simulation chamber so as to have the dielectric front surface of the target at right angles to the axis of the electron beam. The sample is supported by an annular aluminum ring providing electrical contact to the silver-backed Teflon sample through conducting paint. Some 10 cm of the target diameter are unobstructed from front and back so that observations may be readily made. The entire sample holder is placed within but electrically insulated from a grounded enclosure containing an aperture through which the sample is irradiated. By means of this arrangement, the sample edges are not irradiated directly by

the electron beam thus facilitating breakdown studies not dominated by edge effects. Provisions are made to attach potential dividers to the back of the sample, and to insert current probes, electrometers, and Rogowski coils in the sample current paths to ground. The front surface of the sample is visible for inspection and photographic measurements.

During the process of charging the target surfaces, measurements are made of electron beam accelerating potential using a high impedance voltmeter, electron beam current magnitude and distribution over the target area utilizing a rake of five plane current probes with electrometers and chart recorder, and sample charging current employing an electrometer and chart recorder system. Time duration of charging and time to electrical breakdown are recorded to provide a means of estimating the potential to which the target surface has become charged prior to breakdown.

During the electrical discharges which occur at the dielectric targets, short time-duration voltage and current transients are associated with the electrical breakdown. The transient voltages associated with the electrical discharge are measured with a capacitive potential divider. Current transients are measured by a Tektronix CT-1 current probe. Both voltage and current transients are fed through coaxial vacuum-sealed connectors and recorded on a Tektronix 556 oscilloscope. A series of loop antennas 3 cm in diameter and an electronic event counter are used to record electrical signals at various points near the dielectric target during the discharge occurrence.

A system of mirrors and viewing ports permits time-integrated photographs of the self-luminous electrical discharges to be taken. The resultant photographs of the discharge path along the sample surface and the central site of the discharge are correlated with scanning electron microscope studies of material damage.

Charged particle measurements are made using a biased Faraday cup and a retarding potential analyzer (RPA), both of which are illustrated in Fig. 2. The Faraday cup consists of a shielded collector which can be biased to collect either positive or negative particles through a grid aperture of 2.5 cm. The output current of the collector is shunted to ground through a 50 ohm load and the resulting voltage measured with a Tektronix 556 oscilloscope.

The retarding potential analyzer used for the measurement of emitted particles, consists of a particle collector plate and two independently biasable grids enclosed in a grounded shield with an input aperture of 1.2 cm. For the measurement of positive particles the collector is biased at -9 V to capture the positive particles which pass through the grids. Grid G2, the suppressor grid, is biased at -800 V to prevent secondary electron emission from the collector surface which would give rise to erroneous measurements of positive particles. The first grid is then biased positively defining a threshold energy for the incoming particles. By varying the bias on the first grid the energy spectrum of the incoming ions can be measured.

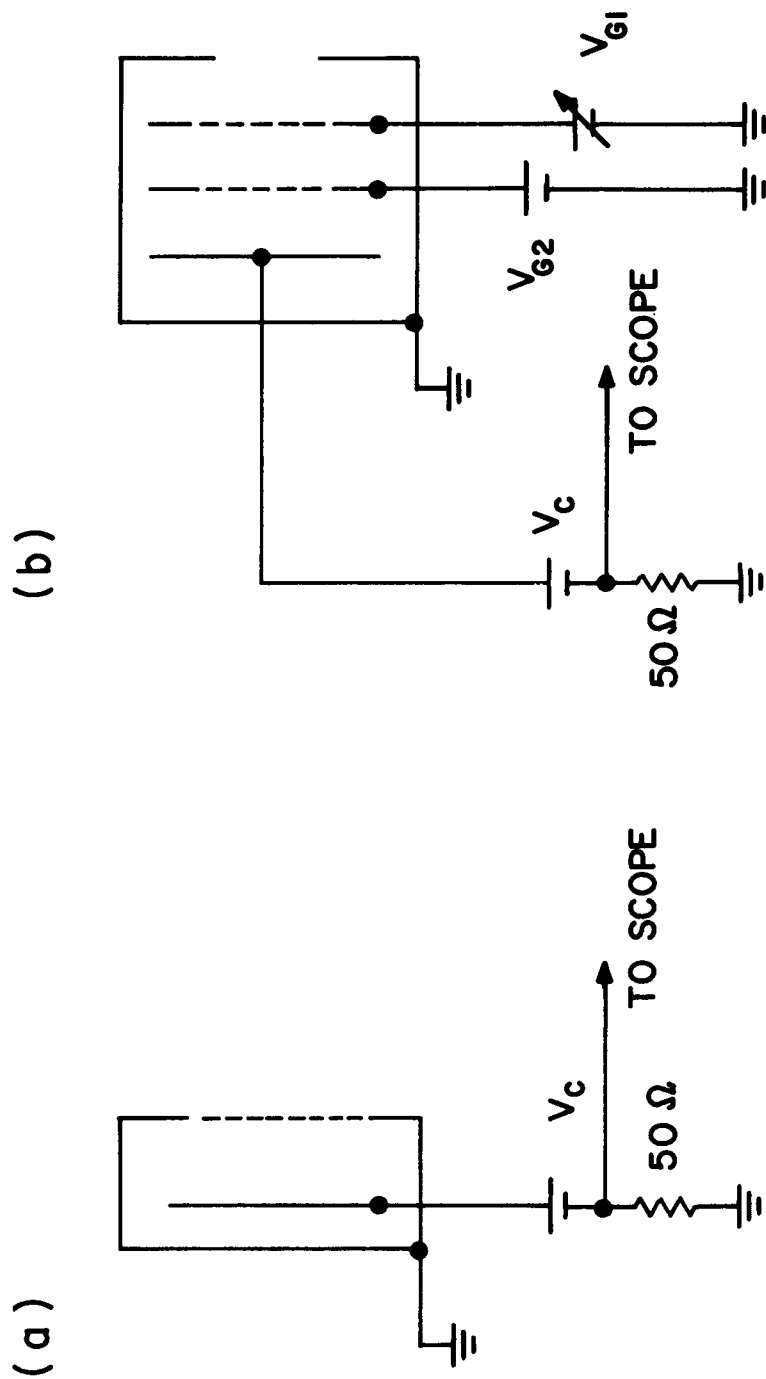


Figure 2. Charged Particle Detectors:

- a) Faraday cup.
- b) Retarding Potential Analyzer.

The output of the collector is measured in a manner identical to that used with the Faraday cup. A temporally-resolved particle flux is thereby derived and particle transit times and total particle emissions are determined.

With the collector biased to + 9 V, the second grid grounded, and the first grid biased negatively, similar measurements are made for negative particles. In all cases the true amplitudes of the incident particles are derived by multiplying the measured signal by the weighting factor of 1.8 which accounts for grid attenuation. The distribution of particle energies is obtained from the measured dependence of collector current on retarding grid voltage by differentiation with respect to grid voltage.

For the angular measurements presented herein, the probes were configured as shown in Fig. 3. The sample is set at $\sim 40^\circ$ to the beam axis to allow observation of normally emitted particles without the detector interfering with the beam. The Faraday cup is set at a fixed angle of 40° below the sample center line and 9.5 cm from the sample surface while the RPA can pivot about the sample 15 cm from the center. The RPA has an angular resolution of 3° assuming a point discharge at the target surface.

3.0 MEASUREMENT TECHNIQUES AND RESULTS

In this section results are first given for the area of Puncture Discharges and Material Damage. This is followed by a somewhat detailed

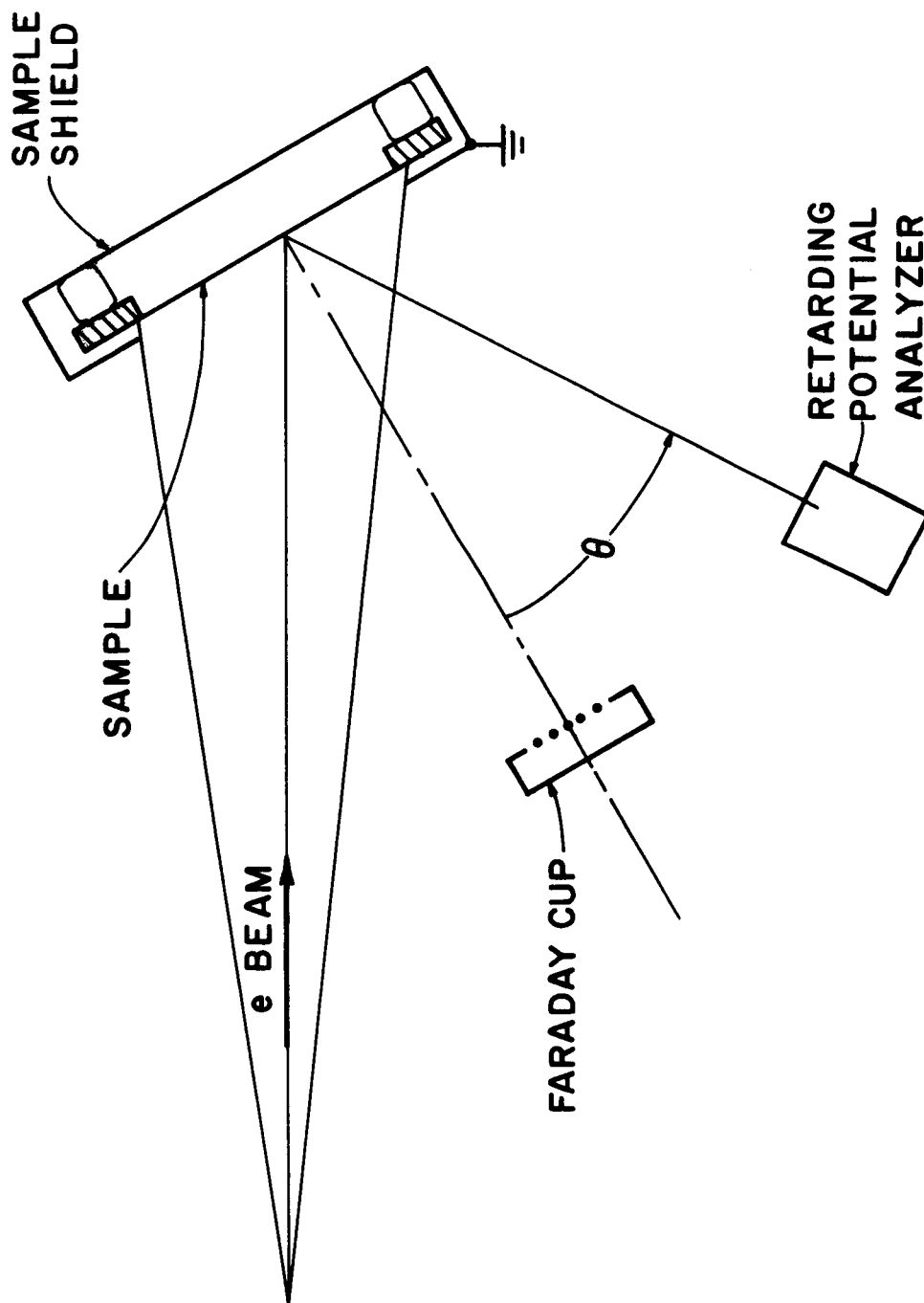
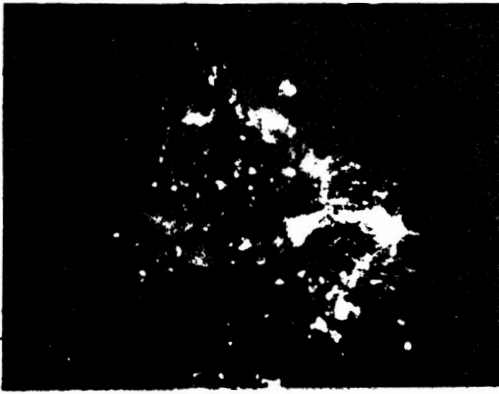


Figure 3. Angular Distribution Measurement System
(Relative orientation of dielectric sample, electron beam and charged particle detectors).

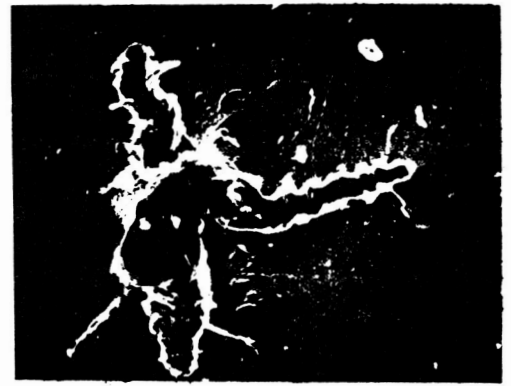
treatment of Charge Particle Emission from the sites of the electrical discharges.

3.1 PUNCTURE DISCHARGES AND MATERIAL DAMAGE

Material damage on the irradiated dielectric surface following an electrical discharge has been studied using an optical microscope and a scanning electron beam microscope (SEM). The optical microscope reveals information about sub-surface damage as well as surface damage while the SEM is used for high resolution surface studies. The photographs in Fig. 4 reveal a hole through the dielectric material to the grounded silver backing resulting from the discharge current flow. In addition, this microscopic investigation reveals the existence of filamentary surface tracks which terminate at the holes as in Fig. 4a and 4b. These material damage tracks are similar in form and appearance to luminous Lichtenberg streamers observed on the surface during the discharge although no direct comparison has been made. The tracks in the Teflon appear to be the results of currents which flow through the Teflon parallel to the surface when the sample is discharged. Ionization and recombination in the current channels are accompanied by light emission which gives rise to the luminous Lichtenberg patterns. The process of discharging the sample by currents flowing underneath the sample surface is consistent with puncture sites where filamentary material damage has occurred as in Fig. 4a and 4b. At other sites as shown in Fig. 4c, where there is no evidence of current channels near the puncture site,



a. Optical micrograph showing subsurface filamentary structure. (100 X)



b. Scanning electron micrograph of breakdown shown in 4a. (250 X)



c. Scanning electron micrograph of non-filamentary breakdown from Teflon side. (300 X)



d. Scanning electron micrograph of damage to silver side. (300 X)

Figure 4. 3 mil silver-backed Teflon sample irradiated at 26 kV with a beam current density of $\sim 1 \text{ nA/cm}^2$.

discharge of the sample occurs by other processes having different electrical paths.

The micro photographs of the discharge sites dramatically demonstrate the material damage resulting from the discharges on the sample. It is evident that the energy in the current channel is sufficient to rupture the channel as in Fig. 4b and to eject molten Teflon from the puncture site. In addition, there is appreciable silver loss from the grounded silver backing as seen in Fig. 4d as well as extensive melting and ejection of material from the discharge sites. The material ejected from the discharge sites in the form of molten material and charged particles is a source of contamination of the spacecraft and its environment.

3.2 CHARGED PARTICLE EMISSION

3.2.1 Measurement Normalization

A correlation technique has been used to compensate for variations in discharge characteristics when measuring either the distribution of particle energies or the angular distribution of emitted particles because the entire distribution cannot be measured during one discharge event. In this approach, the Faraday cup with fixed bias and location serves as a monitor used to normalize the retarding potential analyzer signal. This allows changes in the RPA signal levels associated with changes in angle or energy distribution to be distinguished from variations in discharge characteristic. This procedure allows the

results of certain events to be discarded if a significant departure of the signature on the monitor detector is noted. Since the normalized procedure does not remove variation between different measurements for fixed RPA parameters, an average of three or more normalized events is used to improve the measurement statistics.

3.2.2 Negative Particles

Using the particle detection techniques previously outlined, the time histories of the positive and negative emitted particles were recorded. Traces of the negative particles and positive particles are shown in Fig. 5a and 5b, respectively. The negative trace consists of an early spike followed by a much lower amplitude broader pulse. The early pulse of fast electrons is consistently present for each discharge while the later pulse is present only occasionally. The origin of these signals can be directly ascribed to the collection of particles because the signals are absent if the detector is rotated to a position behind the sample. Also, the signal attributed to positive particles on the RPA can be made to vanish by applying sufficiently positive biases to the retarding energy grid G1 in Fig. 2 while positive particles are still detected on the appropriately biased Faraday cup.

The energy of the early pulse of electrons is measured to be in excess of 3 KeV since a retarding potential of this value did not significantly attenuate the collector current. A determination of the electron energies was not possible since breakdowns in the RPA circuitry

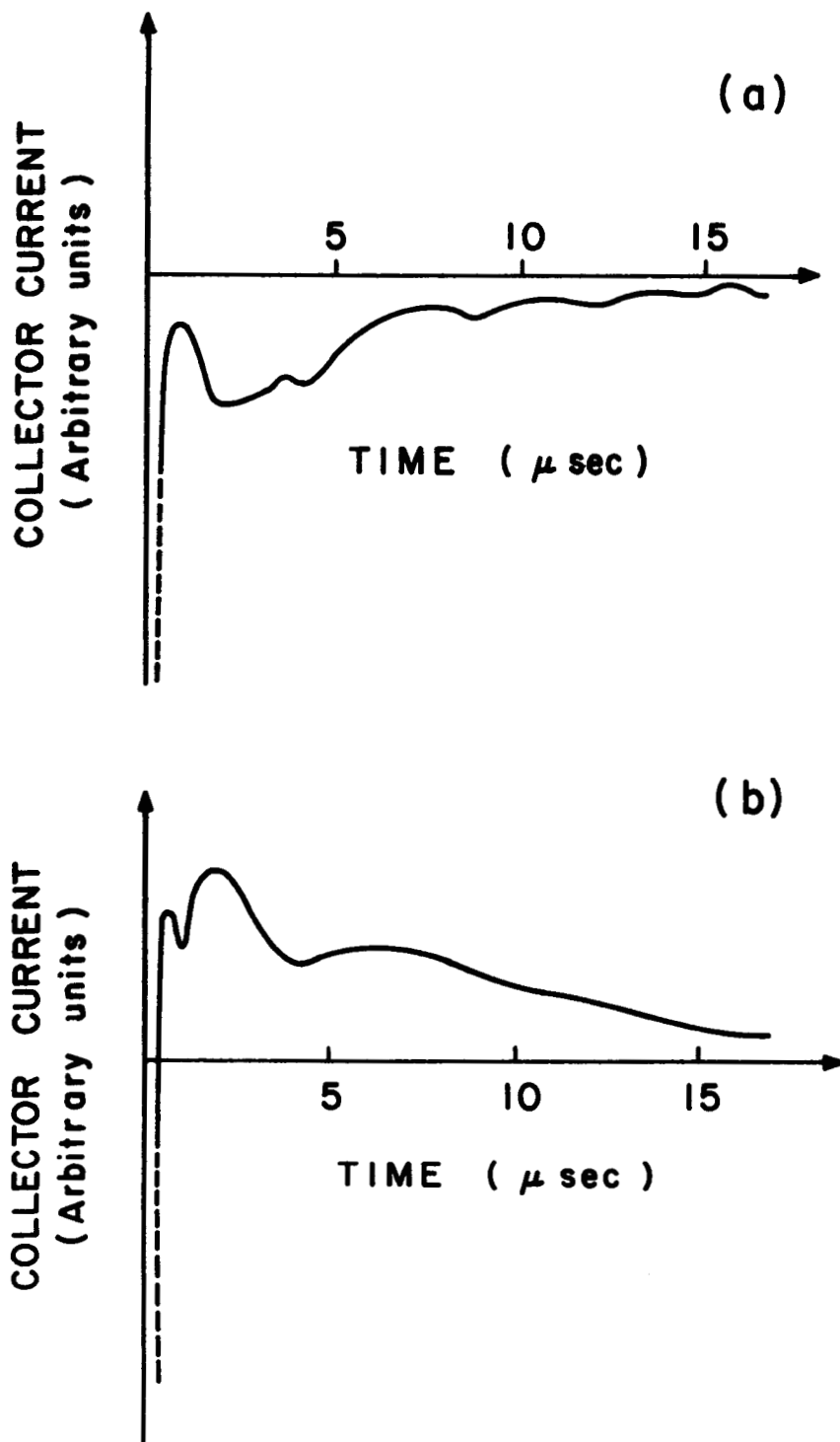


Figure 5. Oscilloscope Traces of Faraday Cup Current:
a) Faraday cup biased to collect negative particles
b) Faraday cup biased to collect positive particles.

prevented applications of voltages in excess of 3 kV. The energy of the later pulse of negative particles is estimated to be less than 85 eV since the application to the Faraday cup of a retarding voltage of this magnitude effectively eliminates this component from the particle flux. The angular distribution of the early pulse of electrons was measured with the RPA biased to collect all negative particles and the results are displayed in Fig. 6. This distribution is strongly peaked in the direction normal to the sample surface, with virtually no particles being observed beyond 45°. Using this distribution as a weighting function, the total number of particles emitted in a given discharge can be determined by measuring the flux emitted at 0° and integrating over the hemisphere through which the particles are emitted. Doing so gives $1-5 \times 10^{13}$ fast electrons emitted during a discharge.

3.2.3 Positive Ions

Investigations of the later positive ion pulse reveal a decrease in intensity of emitted particles as the number of discharge events increases. There is also a tendency for the pulse to disappear after a large number of events. As a result, measurements of the particle energy and angular distributions incorporate a systematic change in character due to repeated breakdowns that cannot be accounted for by averaging a large number of events.

The distribution of particle energies associated with the later positive pulse has been studied immediately after a new sample has been

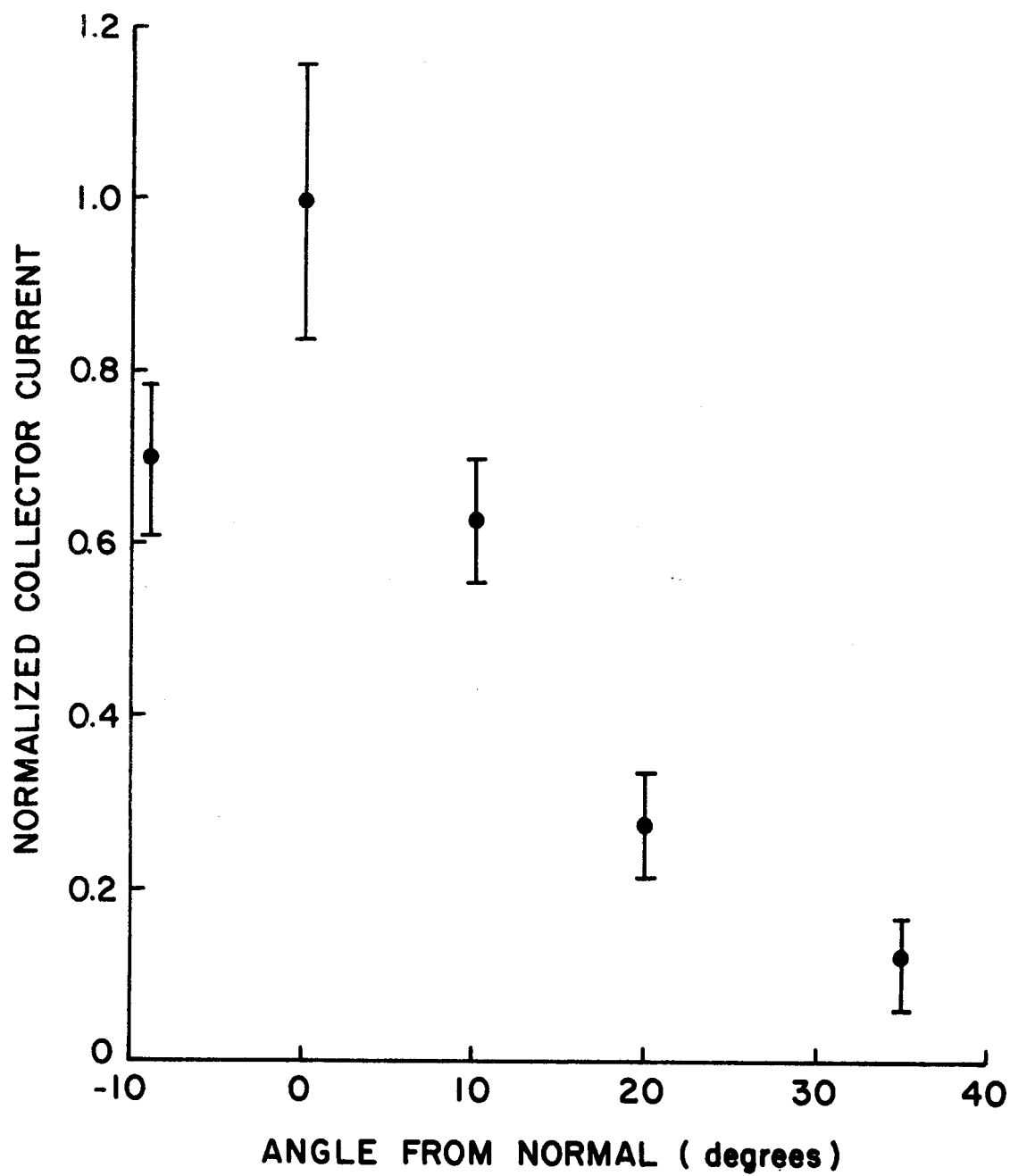


Figure 6. Angular Distribution of Electrons
(For the early burst of electrons emitted during the discharge).

installed for RPA orientation perpendicular to the sample surface. The variation in collector current with retarding grid voltage is presented in Fig. 7 from which the distribution of particle energies $f(E) = Ae^{-\frac{(E-30)}{23}}$ is obtained by differentiation. The results indicate that the particles come off of the sample with a minimum energy of 30 eV. Another estimate of the particle energies can be obtained by determining the time of arrival of the particles at the collector from the temporal evolution of the collector signal. From the transit time and known sample-to-detector distance the velocity, and hence, kinetic energy can be determined. The results again show that all the particles exceed a minimum energy. By equating the minimum energies, an estimate for the positive ion mass can be found if the ion is assumed to be singly ionized. The value of 13.3 amu so obtained is sufficiently close to the atomic weight of carbon 12 to encourage a tentative identification of the later positive ion peaks as due to singly ionized carbon.

The angular distribution of the later positive ion pulse was measured using the procedure outlined above and the results are presented in Fig. 8. The particles are seen to be emitted in a direction nearly normal to the sample surface with a total emission of 7×10^{12} particles per discharge event.

Although no direct measurements of energy distribution or angular distribution of the later negative particles was attempted, it is reasonable to assume that the angular distribution of these particles is similar to the later positive ion distribution in view of the fact

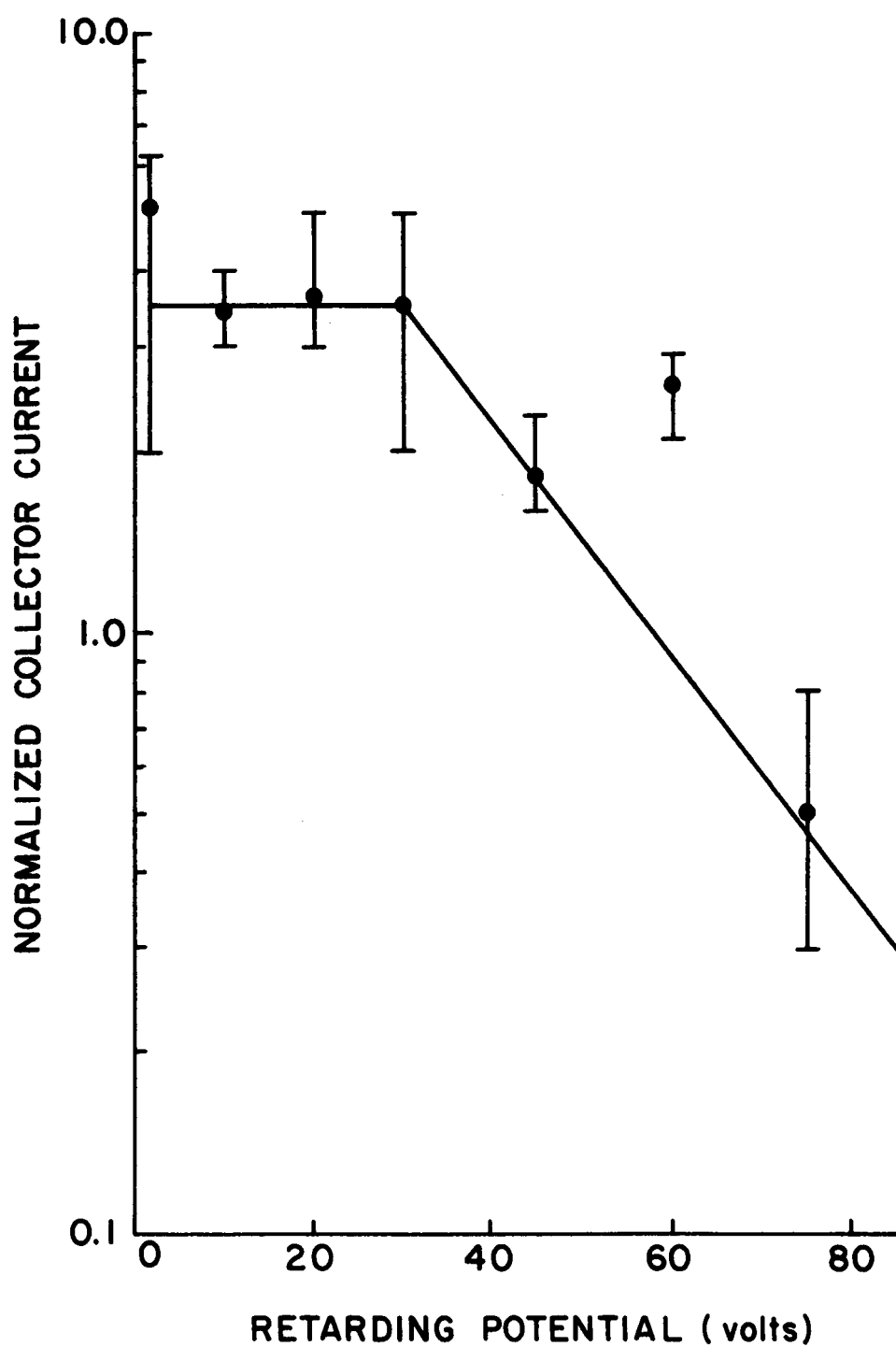


Figure 7. Energy Distribution of Positive Ions Measured with the Retarding Potential Analyzer.

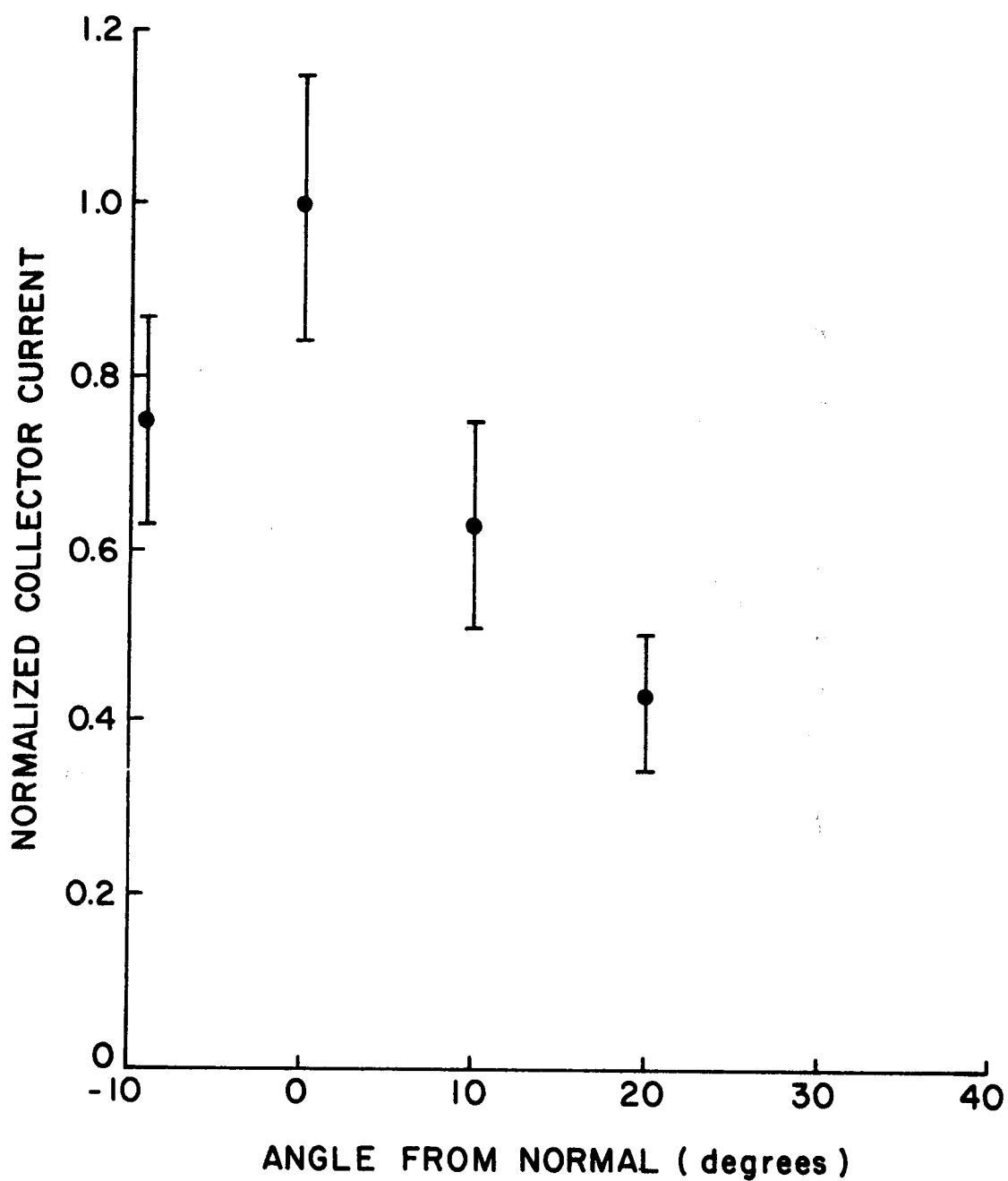


Figure 8. Angular Distribution of Positive Ions Emitted During a Discharge.

that the amplitude and width of these pulses are quite similar. Based on this assumption, the emission of later negative particles is estimated to be $\sim 6 \times 10^{13}$ particles per discharge event.

4.0 DISCUSSION

Material damage resulting from puncture discharges is a source of contamination in spacecraft environments. In addition to expulsion of molten Teflon, emission of charged particles has been observed. The high energy electrons constitute a net loss of 5×10^{13} negative particles from the target per discharge event. The large energies of these particles (in excess of 3 KeV) indicate that the particles are accelerated by the negative voltage of the surface. The presence of later pulses of both positive and negative particles in approximately equal numbers indicates that the particles leave as a plasma with the ions having energies between 30 and 80 eV with a total emission of 10^{13} particles per discharge event.

The redeposition of the molten Teflon can affect performance of nearby solar panels and other sensitive surfaces. Although no direct emission of silver has been detected to date, the loss of silver from the back surface of the thermal control surfaces indicates the presence of silver redeposition on adjacent surfaces. The high energy electrons are expected to leave the negatively charged spacecraft and its immediate environment. The later pulses of positive ions and negative particles are expected to move in the electromagnetic fields of the

spacecraft possibly as a neutral plasma and can be redeposited on adjacent surfaces and affect the response of sensors on the spacecraft. In addition, the emitted particles give rise to electromagnetic disturbances which affect on-board instrumentation.

The results tend to support the observations of Nanevicz and Adamo⁴ and Sessler and West⁵ that electrons are emitted during a discharge. Although the present results indicate a much narrower angular distribution than reported by Nanevicz and Adamo,⁴ this is not surprising in view of the large difference in electron potentials involved.

Further work will be conducted on the emission of charged particles from electrical discharges on simulated spacecraft surfaces in order to identify deposited contaminants and some consideration will be given to alleviation techniques.

4. N. E. Nanevicz and R. C. Adamo, "Malter Discharges as a Possible Mechanism Responsible for Noise Pulses Observed on Synchronous Orbit Satellites," in Spacecraft Charging by Magnetospheric Plasmas (Progress in Astronautics and Aeronautics, Vol. 47) A. Rosen, ed., Cambridge, Mass., MIT Press: 247-261 (1976).
5. B. Gross, G. M. Sessler and J. E. West, "Radiation Hardening and Pressure-Actuated Charge Release of Electron-Irradiated Teflon Electrets," Appl. Phys. Lett. 24 (No. 8):351-353 (1974)

5.0 REFERENCES

1. Spacecraft Charging by Magnetospheric Plasmas, (Progress in Astronautics and Aeronautics, Vol. 47) A. Rosen, ed., Cambridge, Mass., MIT Press (1976).
2. Proceedings of the Spacecraft Charging Technology Conference, eds. C. P. Pike and R. R. Lovell, Air Force Geophysics Laboratory (1977).
3. "Space Radiation Effects (Session D of the Annual Conference on Nuclear and Space Radiation Effects," IEEE Transactions on Nuclear Science, NS-24 (No. 6):2244-2304 (1977).
4. N. E. Nanevicz and R. C. Adamo, "Malter Discharges as a Possible Mechanism Responsible for Noise Pulses Observed on Synchronous-Orbit Satellites," in Spacecraft Charging by Magnetospheric Plasmas (Progress in Astronautics and Aeronautics, Vol. 47) A. Rosen, ed., Cambridge, Mass., MIT Press: 247-261 (1976).
5. B. Gross, G. M. Sessler and J. E. West, "Radiation Hardening and Pressure-Actuated Charge Release of Electron-Irradiated Teflon Electrets," Appl. Phys. Lett. 24 (No. 8):351-353 (1974).